Overview of SIM external calibration

Stuart Shaklan*, Mark Milman, Joseph Catanzarite, Ipek Basdogan, Miltiadis Papalexandris, Lisa Sievers, and Raymond Swartz
Jet Propulsion Laboratory, California Institute of Technology

ABSTRACT

Like all astrometric instruments, the Space Interferometry Mission (SIM) suffers from field-dependent errors requiring calibration. Diffraction effects in the delay line, polarization rotations on corner cubes, and beam walk across imperfect optics, all contribute to field-distortion that is significantly larger than is acceptable. The bulk of the systematic error is linear across the field – that is, it results in a magnification error. We show that the linear terms are inconsequential to the performance of SIM because they are inseparable from baseline length and orientation errors. One approach to calibrating the higher-order terms is to perform 'external' calibration; that is, SIM periodically makes differential measurements of a field of bright stars whose positions are not precisely known. We describe the requirements and constraints on the external calibration process and lay the groundwork for a specific procedure detailed in accompanying papers.

Keywords: Space Interferometry Mission, SIM, interferometry, calibration

1. INTRODUCTION

The Space Interferometry Mission (SIM) is under development in preparation for launch in 2010. The mission's goals are to perform global astrometry of several thousand sources with a precision of ~ 5 micro-arcseconds (uas), and narrow angle (relative) astrometry with a precision of 1 uas. These goals place challenging requirements on the accuracy of SIM's interferometric optical path measurements; for global astrometry, the instrument makes optical path measurements with an accuracy of <1 nm over a range of 2.6 m, while in narrow angle mode, the requirement is 5 times smaller over a range of 17 cm [1]. The dynamic range of the astrometric calibration is likely to be smaller than that of the HST Fine Guidance Sensor (FGS). The FGS performs 0.5 milli-arcsec (mas) astrometry in the presence of 0.5 arcsec systematic errors (dynamic range = 1000) [2]. SIM on the other hand, will calibrate ~ 50 nm errors to a precision of 0.5 nm (dynamic range = 100).

The optical path measurements determine the distance that the starlight travels once it enters the interferometer. The path is measured with a laser beam that is aligned to be parallel to the starlight collected by the interferometer. By definition, the starlight enters the interferometer when the (nominally) planar wave front passes the vertices of the two corner cubes that define the endpoints of the science baseline.

There are many ways that systematic errors cause a false reading of both the metrology and starlight paths as the light propagates from the corner cube planes to the beam combiner. For example, corner cube dihedral errors bias the metrology beam measurement, an effect that depends on the incidence angle of the beam. Beam walk across imperfect optics, caused by slight lateral translations of the delay line or thermal deformations of the structure, results in differential path delays between the starlight and the metrology beam. Polarization, diffraction, aberrations, and other effects are also present. As discussed below and by Sievers et al [3], these effects introduce 10's of nm of systematic optical path errors over the wide-angle field, and a few nm over the narrow-angle field. Sievers et al also demonstrate that the linear component of these errors is inconsequential in wide-angle measurements because they are absorbed by the process of global grid reduction [4]. They may also be inconsequential in narrow-angle measurements, but this depends on how the reference frame and grid stars are used to extract the high-precision information.

* Contact information: Jet Propulsion Laboratory, 4800 Oak Grove Dr., MS 301-486, Pasadena, CA 91109

Our goal in this paper is to discuss a method of on-orbit calibration of the systematic optical path measurement errors. The calibration error c is expressed as a bias to the delay measurement,

$$d = \langle s,b \rangle + c(s,b), \tag{1}$$

where d is the delay, and vectors s and b are the directions to the star and along the baseline, respectively. The symbol $\langle\ \rangle$ represents the inner product. Bias term c is a 2-dimensional function of angle with respect to the baseline, and it has units of distance with a typical magnitude of 10s of nm, as just discussed. It is "locked" to the instrument – that is, it exists only because of instrumental measurement errors. It evolves with time and is not guaranteed to carry pre-launch characteristics into orbit.

We have explored two distinct calibration approaches, called "internal" and "external" calibration. Both are discussed in [3]; here we give a detailed overview of the external calibration approach. This general non-parametric approach relies on differential delay measurements of a grid of bright (V<10) stars. From the differential measurements, a calibration function is estimated, in much the same way that an adaptive optics system uses local tip-tilt measurements to estimate the wave front. In the following section, we describe the calibration procedure, the necessary assumptions behind the approach, the properties of the derived calibration function, the required integration time and noise propagation, and the application of the approach to narrow angle astrometry. The detailed mathematics are left to Papalexandris et al in a separate manuscript [5]. In Sect. 3, we demonstrate that the calibration function is mainly linear in field, but we do not address the issue of high-frequency (1/f ~ 1 wavelength) calibration errors; these are forced to be small through the SIM error budget, and they are being addressed by the technology development program [6]. In Sect. 4, we introduce hybrid calibration approaches that combine the strengths of internal and external calibration

2. EXTERNAL CALIBRATION PROCEDURE

The precise positions of the stars are not known at the beginning of the mission. Given a catalog error of δs, the delay measurement is in error by $\langle \delta s, b \rangle$. Assuming δs =2 mas and b =10 m, the delay error is 100 nm, a few times larger than the uncalibrated instrument bias. Clearly it is not possible to estimate c from raw measurements of stars without a catalog that is accurate to a few uas.

However, if one uses SIM to make differential measurements by changing the baseline by an amount δb while observing a set of stars, then the differential calibration function can be determined as long as is δb reasonably well known. Assume the interferometer is canted by $+\delta b$ for one measurement and $-\delta b$ for another. The differential delay is given by

$$\begin{aligned} \delta d &= \langle s, b+\delta b \rangle + \langle s, b-\delta b \rangle + c(s,b+\delta b) - c(s,b-\delta b) \\ &= \langle s, 2\delta b \rangle + c(s,b+\delta b) - c(s,b-\delta b) \end{aligned} . \tag{2}$$

We want to estimate the c terms across the field-of-regard (FOR) from the difference of the two c terms on the right side of eq. 2. We will first describe the calibration procedure, then return to eq. 2 to estimate the error due to our imperfect knowledge of δb and δs.

Let's choose a set of stars that spans the SIM FOR. From our understanding of the physics of the interferometer (e.g. Kuan et al [7]) we may need just a few stars because c does not have large high-order terms. But to remain more general, and to potentially handle higher order effects due for example to delay line misalignments, we choose a 10x10 or larger grid to cover the circular 15° FOR. To keep integration times reasonable, the stars should all be brighter than V=10. For stars this bright, the delay measurement noise standard deviation is σ_d =140 pm after a 15 s integration. There are plenty of stars available, as shown in fig. 1.

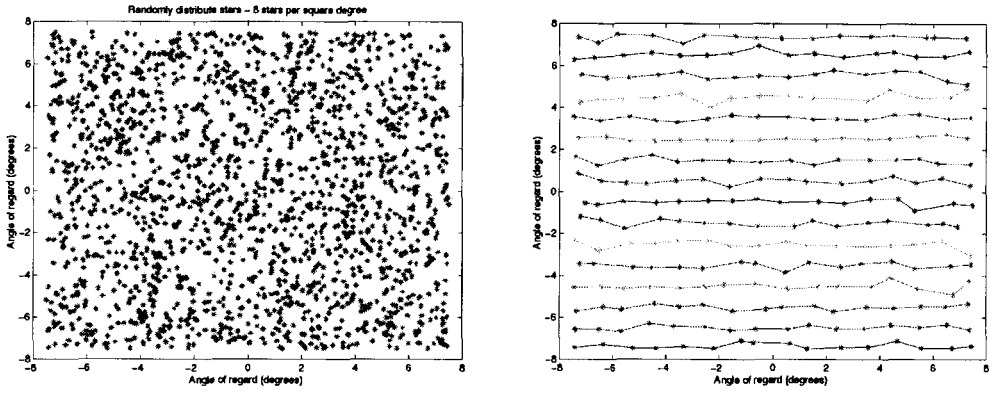

Figure 1. At left, a random field of V<10 stars assuming an average of 8 stars per square degree (mean value for the sky [8]). At right, a 16 x 16 grid selecting the stars that are closest to a uniform grid.

We make 4 measurements of the quasi-regular grid in fig. 1. Defining the baseline to lie on the u-axis, the center of the FOR to be in the z-direction, and the v-axis as z x u, we roll the interferometer about the u-axis by $\pm\delta b$ and cant it by the same amount about the v-axis. The geometry is shown is figure 2.

At each of the 4 baseline positions, SIM measures the entire NxN grid, just as it measures a 'tile' in wide-angle mode. The delay measurements are made in the normal observing mode – therefore they calibrate the instrument in its normal observational state, and they do so without a secondary calibration. A similar process is used with great success to calibrate the HST FGS [2]. While adaptive optics provides a closer mathematical analogy to the SIM external calibration approach, the wave front sensor (e.g. a Shack-Hartman array) contributes a static error due to lenslet imperfections, pixel positions, etc. The sensor calibration (usually performed on a stellar target or internal point source) is critical to performing high-accuracy wave front retrieval. There is no analogous auxiliary sensor used with external calibration.

2.1 Integration time

The time to perform these measurements is computed from the integration time per star and the overhead in setting up each observation. We will integrate on each star for 15 seconds, and conservatively assume 30 seconds of overhead to slew the delay line and acquire a new star. For a grid with 10 stars across the diameter, the total time per baseline orientation is ~1 hr, leading to ~ 4 hours spent performing the calibration. The overhead for calibration may be smaller than the general case because the stars are separated by only 1-1.5 degrees; if the overhead is reduced to 15 s, the total integration time is 2.7 hr.

The amount of time available for calibration is limited to at most 10% of the mission. If the external calibration procedure is to be applied, this places a stability requirement of 1-2 days on the systematic delay error. Many of the key contributors to the systematic error are bound to remain stable for this period of time. Polarization effects related to coatings, and diffraction effects due to clipped apertures are expected to be stable for weeks to months. But other sources of error, particularly those related to thermally driven structural deformations, are more problematic. In Sect. 4 introduce a hybrid approach that updates the changes in c while relying on external calibration for the fundamental calibration.

2.2 Measurement Noise

As noted above, a 15 s integration on a V=10 star yields σ_d =140 pm of shot noise. In addition to this noise, the SIM error budget carries σ_r ~ 200 pm of random noise per measurement associated with metrology, thermal drifts, and other effects. The total noise per measurement is then the root-sum-square of the two terms, ~ 250 pm. We thus carry 250 pm of noise per delay measurement through our simulations.

Our process determines a non-parametric solution to the calibration function. The solution is anchored at the measured grid points. Thus, without placing smoothness constraints on the solution, we expect the 250 pm to represent the approximate noise floor for the calibration process.

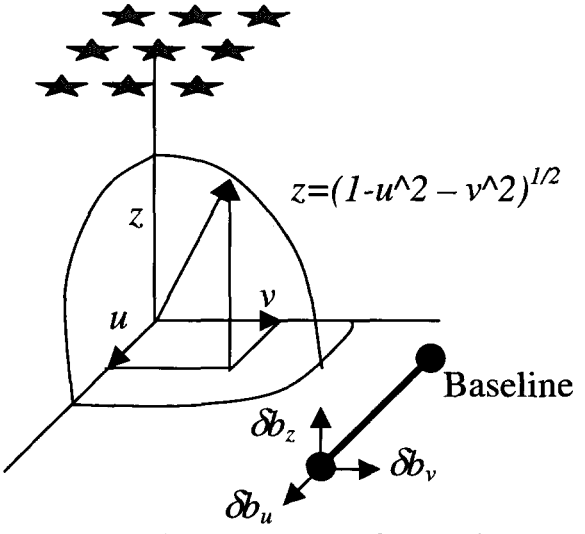

Figure 2. Baseline geometry. The baseline is defined to lie along the *u*-axis. The FOR is centered on the *z*-axis. External calibration is performed by rolling the baseline about the *u*-axis and canting it about the *v*-axis.

To reduce the noise below this level (required for narrow angle calibration but not for wide angle calibration), one may invoke measurement 'chopping,' currently the standard narrow-angle measurement scenario. Chopping implies that we measure for a short period of time (say 15 s) on the target, then move to a reference source in the field, then return to the target and repeat N times. The measurement pairs are differenced to filter long-term drifts (e.g. thermal), reducing linear drift contributions by N, and improving by $\sqrt{N}$ random measurement noise. This technique is being demonstrated in the SIM technology program [9]. The final error per measurement will be commensurate with the narrow angle budget, ~ 40 pm/measurement. This will, of course, increase the integration time per star to ~ 5 minutes, rendering it impractical for large (e.g. 10x10) grids.

2.3 Bootstrapping

SIM is a high-quality astrometric instrument even without astrometric calibration. Its intrinsic ~ 50 nm calibration errors allow it to make 1-2 mas measurements of a field of stars *without* calibration. We take advantage of this by performing an initial measurement of the positions of the external calibration grid stars before beginning the calibration procedure.

A single-tile measurement that does not invoke the wide-angle grid will not get the absolute scale and rotation of the grid stars to better than a part in 10^6 because on-board absolute metrology measures the 10 m baseline length with an accuracy of ~ 10 um. This limitation does not affect calibration (see Sect. 3), but it should be noted that while we are discussing 1-2 mas astrometry of a single tile in the initial calibration bootstrap, we are ignoring the scale and orientation of the calibration grid.

Before any measurements or calibration are performed, the 10 x 10 grid is known to ~ 20 mas (e.g. by ground-based astrometry). After an initial measurement by SIM, the catalog is updated to 2 mas precision. The updated catalog allows SIM to extract calibration results from eq. 2 with an acceptable error. The error in eq. 2 due to δs =2 mas, assuming a $\pm$ 1° baseline cant is given by $\langle \delta s, 2\delta b \rangle$ but δs is tangent to the unit sphere (it contains only *(u, v)* components) while δb is a cant about the *v*-axis, thus it contains primarily a *z* component. Thus $\langle \delta s, 2\delta b \rangle$ << 1 nm. Note that δb =0 for roll about the *u*-axis. The initial uncalibrated star measurement improved the catalog positions to the point that catalog noise is commensurate with other noise sources. The initial cant/roll procedure is then able to estimate the calibration function with a standard deviation of σ_c =500 pm over the FOR. The remaining sources of noise are shot noise, systematic noise, discretization, and interpolation errors.

Another term that degrades the calibration process is the limited knowledge of δb. The guide interferometers are uncalibrated at the start of the mission, limiting our knowledge of cant and roll to δb ~

2 mas. This leads to an error that is bounded by a cubic term in $(\delta b_u + \delta b_v)$ whose amplitude is ~ 1 nm at the edge of the field given the typical calibration errors discussed above [5].

Once an initial tile measurement and an initial calibration measurement are obtained, SIM begins the wide-angle grid-reduction process. The wide-angle grid reduction improves the catalog to δs =100 uas after the first full-sky measurement. At that point, catalog noise is well below the other noise sources. The calibration grid can then be measured with an accuracy limited only by the nature of the calibration function itself (its smoothness and stability), in concert with the granularity and frequency of calibration grid measurements.

2.4 Properties of the External Calibration Function

2.4.1 Smoothness

To successfully derive a calibration function from the differential measurements of eq. 2, the calibration function is expected to be smooth and stable. The temporal stability was discussed in sect. 2.1. The smoothness criterion is related to the coarseness of the grid and the size of the baseline cant. First, any calibration function is acceptable as long as the difference between it and the estimated one is less than the measurement noise, that is

$$\left\| c - \hat{c} \right\|_\infty \le e_c \tag{3}$$

where $\| \|_\infty$ represents the maximum norm. Now the estimation process has both discretization and interpolation errors. From [5], the discretization error is the error due to the existence of high-order derivatives when we make a simple centered differential estimate of $\partial c / \partial u$ from two points. The discretization error in pm/degree is then insensitive to the second derivative and follows

$$e_t = \frac{h^2}{6}\frac{\partial^3 c}{\partial u^3} + \text{high order terms} \tag{4}$$

(and similar for the v derivative), where h is the grid spacing. To maintain this error below the measurement noise, consider 250 pm of measurement noise at h=1° grid spacing. This yields a slope error of 250 pm/degree and places a limit on the third derivative of 1500 pm/cubic degree.

An interpolation error arises between grid points. For simple linear interpolation of our derived estimates of c at the grid points, the interpolation error is given by

$$e_i = \frac{h\Delta u}{2}\frac{\partial^2 c}{\partial u^2} + \text{h.o.t} \tag{5}$$

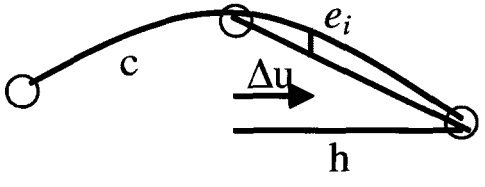

Figure 3. Geometry for calculation of interpolation error.

The geometry is shown in fig. 3. Δu is the distance from a grid point and h is the grid spacing. To maintain e_i <250 pm, with h=1°, the second derivative should obey $\partial^2 c / \partial u^2$ < 1000 pm/sq. degree.

2.4.2 Generality

Smoothness of c as expressed by its 2nd and higher order derivatives affects the accuracy of the estimate. Importantly this is all we demand of c. Its origin is of no consequence to our ability to determine it, except that the physics of its origin affects its smoothness. The calibration function can be caused by the superposition of any number of effects, and there is no requirement that the superposition be linear. The calibration function can take the general form

$$c(u,v) = \sum_{m,n=0,1\ldots} a_m c_1(u,v)^m b_n c_2(u,v)^n \tag{6}$$

and the external calibration function will measure it to within the SIM requirements as long as eqs. 4 and 5 are obeyed and the function is stable ~10 times longer than is required to perform the calibration procedure. For example, the existence of aberrations in the starlight and metrology beams adds to, and potentially couples with, lateral beam walk across imperfect optics. As long as the effects are smooth with field angle, the fractional contributions of each, and any higher order terms related to the product of the individual terms, are rolled into *c(u,v)*. This is in contrast to the proposed internal calibration procedure [3]; for internal calibration, the superposition must be linear ($m,n \leq 1$). Our physical models, however, all indicate that the superposition is in fact linear to a few picometers; we fully expect that non-linearities will not limit the accuracy of internal calibration.

The Hipparcos telescope employed a similar 'external calibration' philosophy to perform on-orbit calibration [10]. The analysis approach used a great-circle reduction to solve for the relationship between on-sky and on-detector directions. They used a simple optical model to account for behavior that could be explained by geometrical effects related to structural deformations, and they found "evidence that certain components of the transformation *cannot* be explained by such structural variations." Thus they were able to model drifts of several milli-arcseconds per year in the instrument while they maintained a model with enough degrees-of-freedom to remove instrument drifts from the astrometric data. This was accomplished using astrometric data collected during the normal course of observation. While this may not be practical for SIM due to the long (> 1 week) period between grid reductions, the end-to-end observation approach combined with a simple model strongly parallels the Hipparcos calibration approach.

3. LINEAR TERMS AND THE CALIBRATION FUNCTION

The SIM flight system is described by Kahn and Aaron [1]. The currently adopted value for the SIM field-of-regard is a 15° diameter circle. Stars are selected by tilting the SIM siderostats over a +/- 3.75° angle, and moving the delay line +/- 1.3m. Corner cubes are attached to the siderostats to retroreflect laser metrology beams that double-pass the delay lines. Now as the corner cubes rotate, the changing incidence angle causes a change in the reflected Stokes parameters that introduces a phase shift on the metrology beam. Since the incidence angle is nominally 20-30 degrees on the corner cube surfaces, and they are rotating by 3.75°, the phase change is mostly linear with field angle. A similar argument can be made for dihedral errors (imperfect corner cube right-angles), as well as the offset distance between the corner cube and the siderostat. Likewise, the metrology and starlight beams propagate ~ 15 m between the siderostats and the beam combiner. Diffraction effects that evolve over the 15 m path will have a large linear change component as the delay line is slewed 1.3 m. Our models (e.g. [7]) show that the bulk of the systematic calibration error is linear in field.

We now explore the implication of the linear terms on the astrometric performance of SIM. SIM makes differential angle measurements within the FOR. The measured delay is given by eq. 1 and the coordinate system is shown in fig. 2. The baseline is known to within an error δb such that the difference between the true baseline b and the estimated one b_o is given by

$$b = b_o + (\delta b_u, \delta b_v, \delta b_z) \tag{7}$$

so that the error one makes in estimating the delay, assuming $c=c_o$ = constant is

$$\delta d = d - d_o = < s, \delta b > = u\delta b_u + v\delta b_v + \sqrt{1-u^2-v^2}\,\delta b_z + c_o \quad , \tag{8}$$

with $(u, v, \sqrt{1-u^2-v^2})$ being the position of a star. When many stars are observed in a tile (that is within the 15° FOR) without resetting the baseline, then eq. 8 forms a matrix $\delta d = Ax$ where the columns of A are the star positions and parameters p are the baseline error 3-vector and the constant term. When many tiles are processed to form a full-sky reduction, then the star positions are written as $s_i = s_{oi} + \delta s_i$ and the δs_i are added to the matrix. This is the basis of the SIM global grid reduction [4].

Now consider the calibration function parameterized as a sum of linear functions and higher order terms,

$$c = c_o + \alpha u + \beta v + c_h(u,v) \ . \tag{9}$$

Substituting this into eq. 2 and expressing the baseline as in eq. 7, we re-write the delay error as

$$\delta d = u(\delta b_u + \alpha) + v(\delta b_v + \beta) + \sqrt{1-u^2-v^2}\,\delta b_z + c_o \tag{10}$$

and it is clear that the linear calibration terms are inseparable from the baseline length and orientation terms. The global grid solution will find a solution to

$$\delta b_u{}' = \delta b_u + \alpha \tag{11}$$

and likewise for the v component. The linear terms do not add any new parameters to the grid solution, and they do not affect the noise propagation or other characteristics of the solution. They are absorbed by the solution, in much the same way that plate-scale and rotation terms are absorbed in relative astrometry at conventional telescopes [11,12].

The implication of this result is that most of the ~50 nm of error in the uncalibrated instrument has no adverse effect on the performance of SIM. The linear terms are of no interest to the calibration process. Returning to the adaptive optics example, we are essentially saying that the sensor does not need to estimate the global tip, tilt, and focus. Below we give two examples illustrating the significance of the result

3.1 Lateral beam walk

Beam walk is a major contributor to the overall SIM error budget, and a significant source of beam walk is attributed to alignment of the delay line rails relative to the metrology beam. SIM carries a beam walk coefficient of 1.6 pm/um assuming lambda/125 r.m.s. optical surfaces. The error grows as the square root of the number of surfaces. Thus, with N~20 arms per surface, each arm of the interferometer picks up ~ 7 pm of optical path error per micron of lateral motion. This implies a tight ~ 10 um alignment of the delay line rails relative to the beam direction. The beam walk error is dominated by spatial frequencies roughly 0.25 – 1 cycle across the metrology beam, or about 0.5 – 2 cm /cycle. Higher frequency errors are averaged by the spatial extent of the beam, while lower frequency errors are common to both starlight and metrology beams.

The beam walk error caused by any lateral motion of the optic is dominated by a term proportional to the beam walk as long as the lateral motion is small compared to the beam diameter, e.g. for a 100 um motion, the beam walk optical path error is mainly the local slope of the 0.5 – 2 cm spatial periods. Thus, for small (< 1 mm) lateral motions caused by misalignment of the delay line rails, the optical path error is a linear function of delay and is therefore proportional to field coordinate u.

This is borne out by simulation. Norbert Sigrist [13] simulated optics having lambda/100 (at 633 nm) r.m.s. surfaces obeying a power spectral density law $f^{-2.5}$. He calculated the average optical path for a metrology beam having a 5 mm diameter at the $1/e^2$ intensity point and plotted the path as a function of lateral beam translation over a 1 mm range (figure 3a). The experiment was repeated 100 times to obtain a meaningful statistical description of the resulting slope sensitivity. He then subtracted the linear terms from each curve and replotted the residuals (figure 3b). While the linear terms had a range of 12 nm (one would expect ~ 16 nm given the 1.6 pm/micron sensitivity figure), the residuals have amplitudes < 1 nm and an r.m.s. of 100 pm. They are clearly dominated by quadratic terms. When the same simulation was run for a total range of 200 nm, the r.m.s. residual was 4 pm, or about 25 times smaller than the 1 mm result (as expected for a quadratic error).

Taking the result for a 200 um misalignment and multiplying by $\sqrt{20}$ to account for the number of optics in the full SIM optical train, one finds that the total non-linear contribution to the SIM error budget assuming straight, misaligned rails is < 20 pm r.m.s. This misalignment figure should be trivial to achieve, as it is ~ 200 urad or 40 arcsec, well within the accuracy of standard theodolites and well within the alignment capabilities for pre- and post-launch integration and test. Should it prove to be non-trivial, even an 80 pm error resulting from a 400 urad misalignment is probably acceptable.

3.2 Corner cube polarization and dihedral errors

Metrology beams suffer phase delays when they encounter dielectric or metallic surfaces such as the gold coating on the SIM corner cubes. The phase delays are dominated by linear terms, as demonstrated by figure 4. For a racetrack beam configuration, with the metrology beam nominally 10 degrees from the (1,1,1) vector, the r.m.s. optical path error is 2.7 nm as the gold-coated cube is articulated over a circular range of 7.5 degrees. After subtracting linear terms, the r.m.s. optical path error is 400 pm (Fig. 4b).

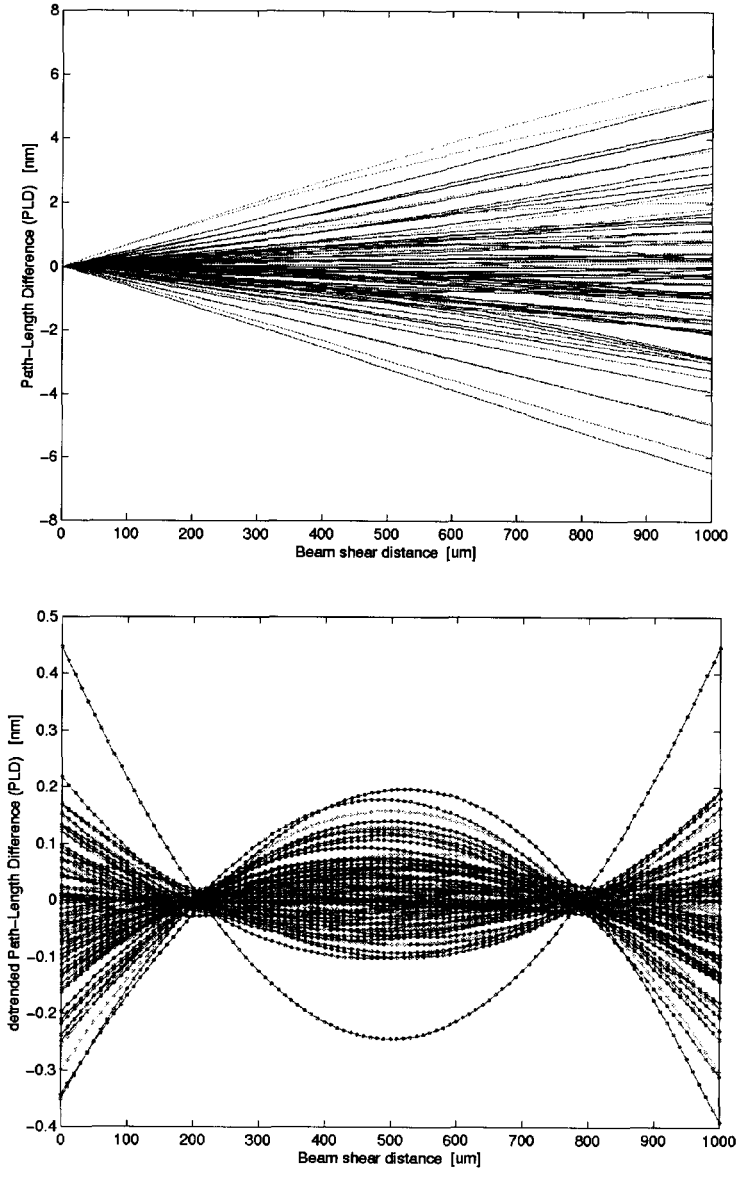

Figure 3. Optical path error resulting from translation of a metrology beam ($1/e^2$ diameter 5 mm) across a lambda/100 surface having an $f^{-2.5}$ power law. (a) shows the optical path error for a 1 mm translation. (b) shows the resulting optical path error after subtracting linear terms. The r.m.s. motion for the curves in (b) is ~100 pm.

Dihedral errors likewise cause largely linear errors, as shown in figure 5. Given a corner cube with a 1 arcsecond (surface) dihedral error, observed at a distance of 10 m with a beam nominally incident at 10 degrees from the (1,1,1) vector, the r.m.s. path error is 4.4 nm as the cube is articulated over a +/- 3.75 degree circle. Figure 5b shows the residual after removing terms linear in u and v. The residual optical path error is 100 pm r.m.s., a factor of 43 reduction compared to the linear terms.

If our polarization and dihedral models represent the true behavior of the SIM corner cubes and metrology beams, then only a factor of 3-5 calibration is required to bring the r.m.s. motion to acceptable levels. Roughly speaking, the r.m.s. optical path error will be 2-3 times the single-beam value for polarization and dihedral errors once one has accounted for external metrology geometry and the number of beams. Given the 1-arcsec corner cubes and angular conditions described above, the r.m.s. error is ~ 1 nm over the SIM field-of-regard after removal of linear optical path terms. Thus, a calibration good to 25% will reduce these errors to < 250 pm.

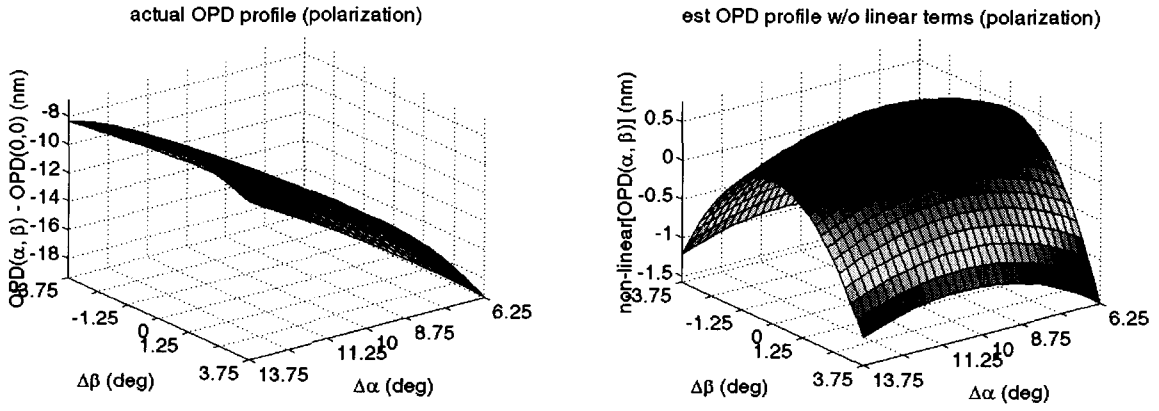

Figure 4. Optical path error resulting from polarization phase shift at a corner cube. A racetrack beam is assumed to hit 3 surfaces in sequence. The beam is nominally 10 degrees from the cube's (1,1,1) vector. (a) shows the raw effect, while (b) shows the residual after removing terms linear in *u* and *v*. Figures provided by Gary Kuan.

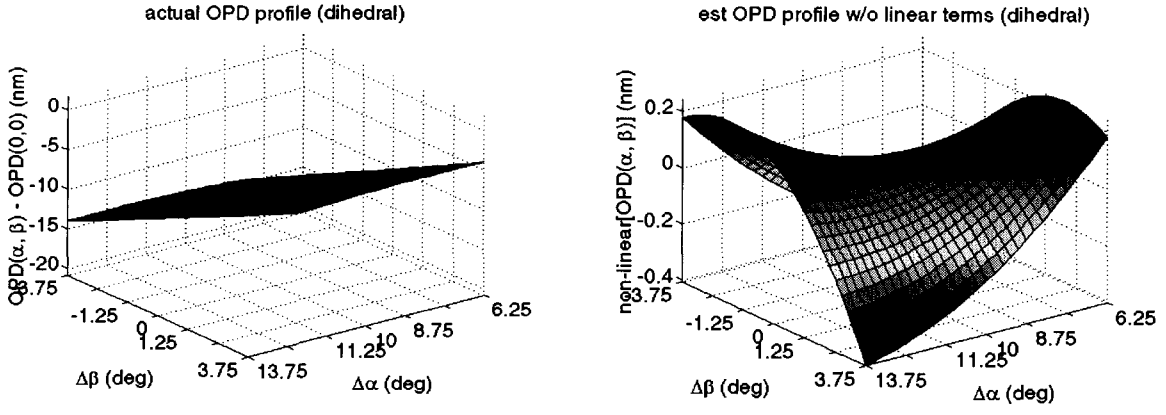

Figure 5. Optical path error resulting from an uncalibrated dihedral error of 1 arcsec on a single face of the corner cube. A racetrack beam is assumed to hit 3 surfaces in sequence. The beam is nominally 10 degrees from the cube's (1,1,1) vector and 10 m from the cube. (a) shows the raw effect, while (b) shows the residual after removing terms linear in *u* and *v*. Figures and simulations provided by Gary Kuan.

4. HYBRID APPROACHES

The external calibration procedure defined in sect. 2 is a general procedure that works well for functions that are have higher-order behavior than our physical models would indicate (e.g. figs 4 and 5). Let's now assume that the physical models are correct in the sense that they describe the smoothness and independence of the calibration function even if they aren't a perfect picometer-for-picometer match to the instrument. That being the case, the polarization and dihedral errors are adequately described by general second-order polynomials, while the beam walk and diffraction terms are separable functions of the delay line position only – that is, they depend on the *u*-coordinate and are independent of *v*. We can then select a much smaller set of stars to perform the calibration, while maintaining a general solution in *u* added to a polynomial across the field. Figure 6 shows the selection of calibration stars to match our model of the calibration function.

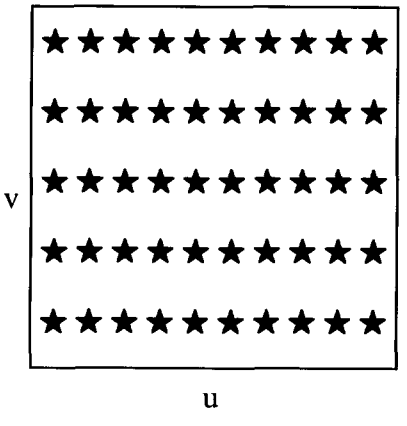

Figure 6. Selection of stars for reduced parameter fit.

The 50 stars are more densely spaced in u with double-spacing in v. This particular set allowed us to utilize our external calibration code to produce an estimated calibration function. However, a set of stars with only one row of dense u-sampling would work well too.

We used the following procedure to estimate the calibration function and force our result to obey the physical model:

1) Perform cant/roll procedure for the 50 stars as described in sect. 2.
2) Use the differential delay measurements to form an estimate $\hat{c}$ as described in ref. 3.
3) Fit a second order polynomial to $\hat{c}$, i.e.

$$c_2(u,v) = au + bv + cuv + du^2 + ev^2 \tag{12}$$

4) From the residual $R(u,v) = \hat{c}(u,v) - c(u,v)$, average the residual over v so that

$$R(u) = \langle R(u,v) \rangle_v \tag{13}$$

5) Estimate the calibration function from the combined polynomial and residuals

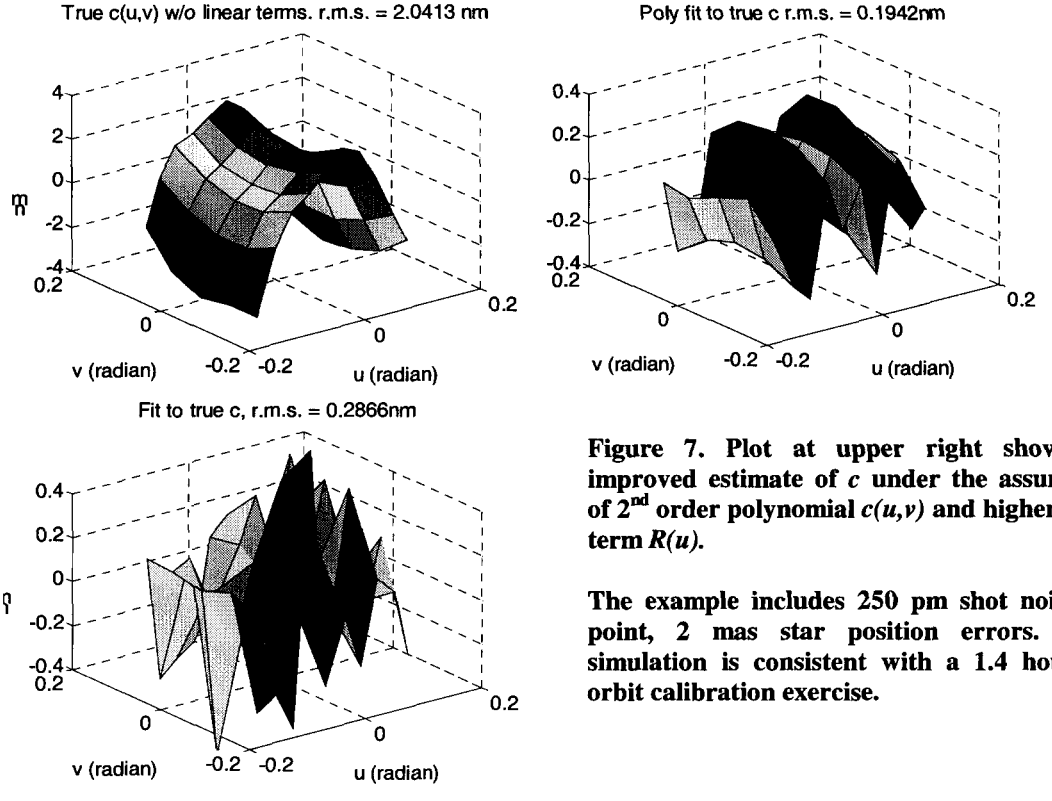

Figure 7. Plot at upper right shows the improved estimate of c under the assumption of 2nd order polynomial $c(u,v)$ and higher order term $R(u)$.

The example includes 250 pm shot noise per point, 2 mas star position errors. The simulation is consistent with a 1.4 hour on-orbit calibration exercise.

$$c(u,v) = c_2(u,v) + R(u) \tag{14}$$

This function is a second order polynomial in (u,v) plus a general function (e.g. piecewise continuous spline with 10 sections) independent of v. Figure 7 shows simulation results for this process. Starting with a model-based calibration function [3], we first derive an estimate $\hat{c}$ shown at lower left in the figure. At upper right we show the final result. The noise level is improved from ~ 300 pm to 200 pm after fitting the polynomial and averaging the residual in v.

Another version of the hybrid approach is to utilize on-board internal calibration modes to measure systematic errors that may change on relatively rapid time scales while relying on external calibration to handle the quasi-static terms. For example, the delay line beam walk terms may change as the structure is deformed by thermal cycling, while the corner cube polarization terms are likely to degrade slowly over the 5 year mission. To apply an internal calibration (i.e. putting the interferometer in retro-reflecting mode and using an on-board laser to measure delay line diffraction and beam walk effects), the calibration function

would be estimated at time $t=t_o$, as above. Also at time $t=t_o$, the internal function $I(u,t_o)$ is measured. At a later time, the internal function is updated, and the new calibration function becomes $c(u,v,t_o)+I(u,t)-I(u,t_o)$. This will correctly update the calibration function as long as changes in I follow changes in c. This is being explored in the SIM testbed program [9].

5. CONCLUSION

The generality of the external calibration solution has important implications for pre-and post launch testing. As discussed in detail in sect. 2.4, the calibration function must be smooth (eqs. 4 and 5) and stable. Thus, the goals of the external-calibration pre-launch test and modeling program are to demonstrate the smoothness and stability of the calibration function. This is in contrast to the internal calibration test program; there the goals are to discriminate the separate terms of the calibration function (e.g. polarization, diffraction, etc.) and apply them to the on-orbit internal calibration over the course of the mission. The two approaches are complimentary in that external calibration gives little insight into the nature of the calibration function, because it is general-purpose. It is slow (it takes hours to complete a calibration) and noisy (250 pm of noise per measurement). Internal calibration on the other hand, forces us to understand exactly how SIM works and places substantial additional requirements on the test program.

The hybrid approaches suggested in sect. 4 provide a compromise. Where the calibration function is smooth and stable, then external calibration is an effective means of deriving c. When the calibration function changes on short time and spatial scales, internal calibration can be used to update the changes.

This research was performed at the Jet Propulsion Laboratory, California Institute of Technology, under contract with the National Aeronautics and Space Administration.

REFERENCES

1. Kahn, P., and Aaron, K, "Space Interferometry Mission: flight system and configuration overview," Proc. SPIE vol. 4852 (Waikaloa, 2002).
2. Benedict, G.F., et al, "Interferometric Astrometry of Proxima Centauri and Barnard's Star Using Hubble Space Telescope Fine Guidance Sensor 3: Detection Limits for Substellar Companions," AJ 118, 108601100 (1999).
3. Sievers, L., et al, "Overview of SIM Calibration Strategies," Proc. SPIE vol. 4852 (Waikaloa, 2002).
4. Swartz, R., "The SIM Astrometric Grid," Proc. SPIE vol. 4852 (Waikaloa, 2002).
5. Papalexandris, M., Milman, M., Shaklan, S., in preparation, based on memo by Papalexandris, M, Milman, M., and Catanzarite, J, "External Calibration Feasibility for SIM," SIM Document Library June 15, 2001.
6. Zhao, F., et al, "Internal metrology beam launcher development for the Space Interferometry Mission," Proc. SPIE vol. 4852 (Waikaloa, 2002).
7. Kuan, G, Moser, S.J., "Sensitivity of Optical Metrology Calibration to Measured Corner Cube Retroreflector Parameters for SIM," Proc. SPIE vol. 4852 (Waikaloa, 2002).
8. Cox, A.N., ed. *Allen's Astrophysical Quantities*, 4th edition AIP Press Springer-Verlag, New York, 2000.
9. Neat, G.W., "The Micro-Arcsecond Measurement Testbed and Its Relationship to the Space Interferometer Mission," Proc. SPIE vol. 4852 (Waikaloa, 2002).
10. Lindegren, L, et al, ``5. Geometrical stability and evolution of the Hipparcos telescope,'' Astron. Astrophys., 258, 35-40 (1992).
11. Eichhorn, H., Williams, C., "On the Systematic Accuracy of Photographic Astrometric Data," AJ 68,221-231 (1963).
12. Shaklan, S., Milman, M., and Pan, X., "High-Precision Early Mission Narrow-Angle Science with the Space Interferometry Mission," Proc. SPIE vol. 4852 (Waikaloa, 2002).
13. Sigrist, N., private communication, 2001.